



NOVA

University of Newcastle Research Online

nova.newcastle.edu.au

Hyder, Md Mashud; Khan, Reduan H; Mahata, Kaushik "An enhanced random access mechanism for Smart Grid M2M communications in WiMAX networks" Published in Proceedings of the 2014 IEEE International Conference on Smart Grid Communications (SmartGridComm) (Venice, Italy 03-06 November, 2014) p. 356-361 (2015)

Available from: <http://dx.doi.org/10.1109/SmartGridComm.2014.7007672>

© 2015 IEEE. Personal use of this material is permitted. Permission from IEEE must be obtained for all other uses, in any current or future media, including reprinting/republishing this material for advertising or promotional purposes, creating new collective works, for resale or redistribution to servers or lists, or reuse of any copyrighted component of this work in other works.

Accessed from: <http://hdl.handle.net/1959.13/1339415>

An Enhanced Random Access Mechanism for Smart Grid M2M Communications in WiMAX Networks

Md Mashud Hyder, Reduan H. Khan, and Kaushik Mahata
School of Electrical Engineering and Computer Science
The University of Newcastle, NSW 2308, Australia

Abstract—Random access is being considered as one of the key bottlenecks for supporting machine-to-machine (M2M) communications over an IEEE 802.16-based WiMAX network. Apart from handling massive access attempts from a large number of devices, the random access plane requires service differentiation capability to meet the diverse QoS requirements of various M2M applications. To address these issues, in this paper, we propose an enhanced random access scheme, where the fixed/low-mobility M2M devices pre-equalize their random access codes using the estimated frequency response of the slowly-varying wireless channel. Consequently, the base station is able to detect a large number of codes as their mutual orthogonality remains preserved. Moreover, a differentiated random access strategy is proposed to provide QoS-aware access service to various M2M devices. The performance of the proposed scheme is demonstrated under two different code matrices using both theoretical analysis and simulation results.

Index Terms—WiMAX, M2M, QoS, Random Access.

I. INTRODUCTION

In a Smart grid environment, a WiMAX network has to support a large number of fixed/low-mobility machine-to-machine (M2M) devices that will transmit bursty, small data packets (e.g., meter readings and sensor reports) under a valid security association with the network [1]. This corresponds to a heavily uplink-biased traffic model following a Poisson distribution. Random access based bandwidth request (BR) is preferable for such traffic, which exploits the benefits of statistical multiplexing to support a large number of devices at a fixed overhead. However, the unique characteristics of M2M communications pose two key challenges to the existing WiMAX random access mechanism. First, the random access channels perform optimally when the number of devices contending simultaneously do not exceed a particular threshold. Otherwise, the channel becomes unstable in terms of access success rate and access delay. Moreover, apart from the high perennial random access load, the number of simultaneously contending devices may increase rapidly due to a certain fault/outage event [2]. This may in turn congest the whole random access plane, resulting in heavy packet-loss and prolonged delay. Second, in the existing IEEE 802.16 standards, only a single QoS scheduling class, i.e. the Best Effort (BE) service is associated with random access mechanism. Therefore, it is not possible to provide differentiated access service to various M2M devices/applications using the conventional BE service.

A simple solution of this problem is to increase the number of BR channels to accommodate more users/devices. However, under the existing schemes, only a handful of codes can be detected reliably per channel per frame in presence of multiple access interference (MAI) from different codes, as well as random noise and fading in the multipath wireless channel [3]. Therefore, a lot of BR channels are required, which would substantially reduce the payload capacity of the overall system. Hence, random access has been considered as one of the key bottlenecks by the IEEE 802.16p working group for M2M communications. To overcome this limitation, the recent IEEE 802.16p amendment has proposed several solutions, mostly based on access control over the MAC layer [4]. On the other hand, a number of works have already appeared in the literature concerning this problem, e.g., [5] and [6]. However, these schemes require significant modification to the existing standards and are not suitable for a network supporting both M2M and non-M2M traffic.

Since in a Smart Grid environment, most of the M2M devices are either fixed or have very low-mobility, their wireless channels are expected to experience only a small variation in time. The Doppler spectrum for such a channel has a rounded shape with zero mean which yields a large coherence time [7]. Based on this unique feature of M2M traffic, in this paper, we propose an enhanced random access scheme, where the fixed/low-mobility M2M devices pre-equalize their BR codes using the estimated frequency response of their slowly-varying channels; consequently, the base station (BS) is able to detect a large number of codes as their mutual orthogonality remains preserved. Mathematical analysis is carried out to determine the theoretical performance limit of the code detector. The analysis reveals that the default Pseudo-random code matrix specified in the IEEE 802.16 standard is not quite effective for detecting a large number of codes under the proposed scheme. As a remedy, we argue that a Hadamard code matrix can significantly increase its code detection performance. Moreover, a differentiated random access strategy is proposed to provide QoS-aware access service to various M2M devices. The theoretical performance of the proposed scheme is validated by simulation results under both of the two code matrices.

The rest of the paper is organized as follows. Section II describes the system model and the key tenets of the proposed random access mechanism. Section III formulates the concept of differentiated random access strategy. Simulation results are provided in Section IV, followed by conclusions in Section V.

II. SYSTEM MODEL

Consider a single-cell WiMAX network with time division duplex (TDD) OFDMA physical layer. A BR channel is comprised of $L = 144$ randomly chosen subcarriers over one OFDM symbol. A BR code is a L -bit pseudo random binary sequence (PRBS) chosen with equal probability from a bank of K codes, where $K \leq 256$ [8]. For rest of the sequel, let us denote the BR code-matrix as $\mathbf{C} \in \mathbb{R}^{L \times K}$. A component of \mathbf{C} is indicated by $\mathbf{C}_{l,k}$, where $l = 1, 2, \dots, L$ and $k = 1, 2, \dots, K$; and the k^{th} column of \mathbf{C} represents an independent code denoted by \mathbf{C}_k . For random access, a subscriber station (SS) picks a random column from the code matrix $\mathbf{C} \in \mathbb{R}^{L \times K}$ and transmits it onto the BR channel by BPSK modulating each of its L subcarriers, i.e. $\mathbf{C}_{l,k} \in \{-1, +1\}$.

A. Pre-Equalization

The first OFDM symbol of each WiMAX frame is a preamble transmitted by the BS, where the subcarriers are BPSK modulated with a boosted pilot sequence [8]. Typically, the SSs use this information to estimate the channel frequency response (CFR) for the OFDM demodulation process. Since all the SSs are already time-synchronized through the ranging process, a SS can pre-equalize its BR code using this estimated CFR exploiting the channel reciprocity of the TDD system [9]. A number of pre-equalization techniques are available. For more details, please refer to [10].

Now, consider a time instant where M number of SSs are simultaneously contending on the same BR channel. Let, the m^{th} SS selects the k_m^{th} column of the code matrix $\mathbf{C} \in \mathbb{R}^{L \times K}$, where $m = 1, 2, \dots, M$. Considering zero-forcing (ZF) pre-equalization [10], the transmitted code over the l^{th} subcarrier from the m^{th} SS be

$$x_{l,m} = \frac{\mathbf{C}_{l,k_m}}{\hat{h}_{l,m}} \text{ for } \forall l \in \{1, 2, \dots, L\}, \quad (1)$$

where $\hat{h}_{l,m}$ is the pilot-aided CFR estimated by the m^{th} SS. To be more precise, $\hat{h}_{l,m}$ can be expressed as

$$\hat{h}_{l,m} = h_{l,m} + e_{l,m}, \quad (2)$$

where $h_{l,m}$ is the actual frequency response of the l^{th} subcarrier and $e_{l,m} \sim \mathcal{CN}(0, \sigma_{e,m}^2)$ is a zero-mean complex Gaussian noise.

In the BS, after down-conversion to baseband and OFDM demodulation, the received signal from the m^{th} SS over the l^{th} subcarrier be

$$y_{l,m} = x_{l,m} \bar{h}_{l,m} = \mathbf{C}_{l,k_m} \frac{\bar{h}_{l,m}}{\hat{h}_{l,m}} \text{ for } \forall l \in \{1, 2, \dots, L\}, \quad (3)$$

where $\bar{h}_{l,m}$ is the effective channel experienced by the SS.

Note that, although the position of the BS and the SS are fixed for stationary M2M devices, the channel is continually affected by the movement of the external scatterers in the surrounding environment [7]. Consequently, $\bar{h}_{l,m}$ will differ from $h_{l,m}$. To generalize, assume the effective channel can be modeled as [11]

$$\bar{h}_{l,m} = \alpha h_{l,m} + \eta_{l,m}, \quad (4)$$

where $\eta_{l,m} \sim \mathcal{CN}(0, \sigma_{\eta,m}^2)$ is a zero-mean complex Gaussian noise and α is some deterministic complex valued constant. Considering the above phenomena, the combined received signal at BS from all M stations over the l^{th} subcarrier be

$$y_l = \sum_{m=1}^M \left\{ \mathbf{C}_{l,k_m} \frac{\alpha h_{l,m} + \eta_{l,m}}{h_{l,m} + e_{l,m}} \right\} + \vartheta_l, \quad (5)$$

where $\vartheta_l \sim \mathcal{CN}(0, \sigma_{\vartheta}^2)$ is a zero-mean complex Gaussian noise. Equation (5) can be represented as

$$y_l = \sum_{m=1}^M \left\{ \mathbf{C}_{l,k_m} - \lambda_{l,m} \mathbf{C}_{l,k_m} \right\} + \vartheta_l, \quad (6)$$

where $\lambda_{l,m}$ is a ratio of complex variables, i.e.

$$\lambda_{l,m} = \frac{(1 - \alpha)h_{l,m} + e_{l,m} + \eta_{l,m}}{h_{l,m} + e_{l,m}} \quad \forall l \quad (7)$$

Let us construct

$$\mathbf{y} = [y_1, y_2, \dots, y_L]^T, \quad (8)$$

where $(\cdot)^T$ denotes transpose of a vector.

B. Code Detection

To detect the presence of a BR code, the code detector in the BS correlates the received signal with a matching matrix $\mathbf{D} \in \mathbb{R}^{L \times K}$. The detector takes every column of \mathbf{D} and computes its cross-product with \mathbf{y} . The design principle of \mathbf{D} should be such that i) the correlation between p^{th} column of \mathbf{D} , i.e. \mathbf{D}_p and \mathbf{C}_p is maximized and, ii) the correlation between \mathbf{D}_p and \mathbf{C}_{k_m} with indices $k_m \neq p$ is minimized. Let the detector picks a random column p denoted as \mathbf{D}_p , where $p = 1, 2, \dots, K$. The corresponding result of cross-product would be

$$\mathbf{D}_p^T \mathbf{y} = \sum_{l=1}^L \left\{ \sum_{m=1}^M \left\{ \mathbf{C}_{l,k_m} \mathbf{D}_{l,p} - \lambda_{l,m} \mathbf{C}_{l,k_m} \mathbf{D}_{l,p} \right\} + \vartheta_l \mathbf{D}_{l,p} \right\} \quad (9)$$

For code detection, the detector checks the probability density function (PDF) of $\mathbf{D}_p^T \mathbf{y}$ and decides in favour of one of the following two hypotheses - i) \mathcal{H}_0 : the code \mathbf{C}_p is not present in \mathbf{y} , and ii) \mathcal{H}_1 : the code \mathbf{C}_p is present in \mathbf{y} . The code detector applies this strategy individually for every $\mathbf{D}_p : p \in \{1, 2, \dots, K\}$ in (9).

As mentioned earlier, in this work, we consider two different matching matrices. The first one is the default Pseudo-random code matrix defined in the IEEE 802.16 standard, which provides K number of nearly orthogonal codes. The other one is generated from partial Hadamard code matrix. The detection performance of these two matrices are analyzed in the following subsections.

Case A: Pseudo-Random Code Matrix

We consider $\mathbf{D} = \mathbf{C}$. Under this case, if \mathcal{H}_0 is true, then (9) follows

$$\mathbf{C}_p^T \mathbf{y} = \sum_{l=1}^L \sum_{m=1}^M \mathbf{C}_{l,k_m} \mathbf{C}_{l,p} - \sum_{l=1}^L \sum_{m=1}^M \lambda_{l,m} \mathbf{C}_{l,k_m} \mathbf{C}_{l,p} + \sum_{l=1}^L \vartheta_l \mathbf{C}_{l,p} \quad (10)$$

Otherwise, under \mathcal{H}_1

$$\begin{aligned} \mathbf{C}_p^T \mathbf{y} = & L - \sum_{l=1}^L \lambda_{l,m} + \sum_{l=1}^L \sum_{m=1, k_m \neq p}^M \mathbf{C}_{l,k_m} \mathbf{C}_{l,p} \\ & + \sum_{l=1}^L \sum_{m=1, k_m \neq p}^M \lambda_{l,m} \mathbf{C}_{l,k_m} \mathbf{C}_{l,p} + \sum_{l=1}^L \vartheta_l \mathbf{C}_{l,p} \end{aligned} \quad (11)$$

In order to carry out the hypothesis test, we need to obtain the probability density function of $\mathbf{C}_p^T \mathbf{y}$ under the hypothesis \mathcal{H}_ℓ for $\ell = 0, 1$. At first, we consider \mathcal{H}_0 . Let us consider (6). If there was no channel estimation error i.e. $\lambda = 0$, the whole energy of the users will be only in the real part of \mathbf{y} , and the imaginary part will contain only noise. Moreover, in the R.H.S. of (10), the first term $\sum_{l=1}^L \sum_{m=1}^M \mathbf{C}_{l,k_m} \mathbf{C}_{l,p}$ is real-valued and its variance is much larger than the other two terms. Hence, we can consider the real part of $\mathbf{C}_p^T \mathbf{y}$ only.

By using the central limit theorem, the distribution of $\sum_{l=1}^L \sum_{m=1}^M \mathbf{C}_{l,k_m} \mathbf{C}_{l,p}$ can be approximated as a normally distributed random variable with zero mean and variance ML . Similarly, since ϑ_l is modeled as random variable with complex Gaussian distribution, we can approximate distribution of $\Re \left[\sum_{l=1}^L \vartheta_l \mathbf{C}_{l,p} \right]$ using a normally distributed random variable with zero mean and variance $L\sigma_\vartheta^2/2$. According to (7), $\lambda_{l,m}$ is a ratio of two complex quantities. Similar to [11], the quantity $\lambda_{l,m}$ can be modeled using a random variable $\lambda = \lambda_r + i\lambda_i$ with PDF

$$f(\lambda_r, \lambda_i) = \frac{(1 - |\rho|^2) \sigma_u^2 \sigma_v^2}{\pi} (\sigma_v^2 (\lambda_r^2 + \lambda_i^2) + \sigma_u^2 - 2\rho_r \lambda_r \sigma_u \sigma_v + 2\rho_i \lambda_i \sigma_u \sigma_v)^{-2}, \quad (12)$$

where $\sigma_u^2 = |1 - \alpha|^2 \sigma_{h,m}^2 + \sigma_{e,m}^2 + \sigma_{\eta,m}^2$, $\sigma_v^2 = \sigma_{h,m}^2 + \sigma_{e,m}^2$, and $\rho = (1 - \alpha) \sigma_{h,m}^2 + \sigma_{e,m}^2$. In Appendix-A, we derive the mathematical expectation and variance of λ_r , i.e. μ_r and σ_r^2 respectively.

Remark 1. In practice, the variance of channel frequency response, i.e. $\sigma_{h,m}^2$ may be different for $m = 1, 2, \dots, M$. However, the BS always equalizes the channel power of the active users through the ranging procedure, where the channel power can be expressed by $\frac{\|\mathbf{h}_m\|^2}{L}$ with $\mathbf{h}_m = [h_{1,m}, h_{2,m}, \dots, h_{L,m}]^T$. Again, if the CFR is modeled as a complex Gaussian random variable then channel power can be approximated by its variance. Hence, the variance must remain in a known interval due to the ranging process. Consequently, we can use the value of average channel power as an estimate of $\sigma_{h,m}^2$ for all m . Similarly, BS can estimate $\sigma_{e,m}^2$ and $\sigma_{\eta,m}^2$.

By using *Remark-1* and the central limit theorem, the distribution of $\Re \left[\sum_{l=1}^L \sum_{m=1}^M \lambda_{l,m} \mathbf{C}_{l,k_m} \mathbf{C}_{l,p} \right]$ can be modeled as a normally distributed random variable with mean zero and variance $LM\sigma_r^2$. Thus, under the hypothesis \mathcal{H}_0 , the distribution of $\Re \left(\mathbf{C}_p^T \mathbf{y} \right)$ can be approximated as a random variable with zero-mean Gaussian distribution and variance σ_0^2 , where $\sigma_0 = \sqrt{L\sigma_\vartheta^2/2 + ML + LM\sigma_r^2}$. Similarly, under the hypothesis \mathcal{H}_1 , the distribution of $\Re \left(\mathbf{C}_p^T \mathbf{y} \right)$ can be approximated by a normally distributed random variable with mean L and variance σ_1^2 , where $\sigma_1 = \sqrt{L\sigma_\vartheta^2/2 + (M-1)L + LM\sigma_r^2}$.

Next, we set a threshold ξ such that decision statistics for p^{th} correlation yields $|\Re \left(\mathbf{C}_p^T \mathbf{y} \right)| \lesssim_{\mathcal{H}_0}^{\xi} \xi$. Thus, the probability of false alarm be

$$P_f^{(p)} = P \left(|\Re \left(\mathbf{C}_p^T \mathbf{y} \right)| > \xi | \mathcal{H}_0 \right) \quad (13)$$

Note that, the random variable $|\Re \left(\mathbf{C}_p^T \mathbf{y} \right)|$ has a folded normal distribution. Hence, its cumulative distribution function (CDF) can be defined as

$$F(z) = P \left(|\Re \left(\mathbf{C}_p^T \mathbf{y} \right)| \leq z \right) = \text{erf} \left(z / \sqrt{2\sigma_0^2} \right)$$

where $\text{erf}(x)$ is the standard error function. Then (13) becomes

$$P_f^{(p)} = P \left(|\Re \left(\mathbf{C}_p^T \mathbf{y} \right)| > \xi | \mathcal{H}_0 \right) = 1 - \text{erf} \left(\xi / \sqrt{2\sigma_0^2} \right) \quad (14)$$

Let we want to select a threshold ξ_ϕ such that the desired false alarm probability $P_f^{(p)} = \phi$. Then one have the relation

$$1 - \text{erf} \left(\xi_\phi / \sqrt{2\sigma_0^2} \right) = \phi. \quad (15)$$

Note that, the value of ϕ indicates the probability of $|\Re \left(\mathbf{C}_p^T \mathbf{y} \right)|$ goes above ξ_ϕ under the hypothesis \mathcal{H}_0 . If any $\{ |\Re \left(\mathbf{C}_p^T \mathbf{y} \right)| \}_{p=1}^L$, that should be under \mathcal{H}_0 , goes above ξ_ϕ then we get false alarm. Then the overall false alarm probability can be defined as

$$P_f = 1 - (1 - \phi)^{L-M} \quad (16)$$

Similarly, the probability of detection for the p^{th} correlation under \mathcal{H}_1 be

$$\begin{aligned} P_d^{(p)} &= P \left(|\Re \left(\mathbf{C}_p^T \mathbf{y} \right)| > \xi | \mathcal{H}_1 \right) \\ &= 1 - \frac{1}{2} \left[\text{erf} \left(\frac{\xi + L}{\sqrt{2\sigma_1^2}} \right) + \text{erf} \left(\frac{\xi - L}{\sqrt{2\sigma_1^2}} \right) \right] \end{aligned} \quad (17)$$

Since a detection will only be successful when all M terms of $\{ |\Re \left(\mathbf{C}_p^T \mathbf{y} \right)| \}_{p=1}^L$ that are in \mathcal{H}_1 goes above ξ , we can write

$$P_d = \left(P_d^{(p)} \right)^M \quad (18)$$

Case B: Hadamard Code Matrix

In general, the detector cannot detect large number of active users by using the Pseudo-random code matrix. On the detection process under \mathcal{H}_1 for a particular active code \mathbf{C}_p , the algorithm treats the contribution of other active codes as additional noise without attempting any mitigation of MAI. Moreover, when we correlate \mathbf{y} with \mathbf{C}_p , the variance of other noise terms $(\sum_{l=1}^L \vartheta_l \mathbf{C}_{l,p} - \sum_{l=1}^L \sum_{m=1}^M \lambda_{l,m} \mathbf{C}_{l,k_m} \mathbf{C}_{l,p})$ also increases. The process results in performance degradation as the number of subscribers increase. To overcome these limitations, we apply partial Hadamard matrix as a code matrix \mathbf{C} . We first construct a Hadamard matrix of order 256, then retain its upper left block of size $L \times L$ as \mathbf{C} . The matching matrix is constructed as $\mathbf{D} = (\mathbf{C})^{-1}$.

Under this case, if \mathcal{H}_0 is true, then (9) follows

$$\mathbf{D}_p^T \mathbf{y} = - \sum_{l=1}^L \sum_{m=1}^M \lambda_{l,m} \mathbf{C}_{l,k_m} \mathbf{D}_{l,p} + \sum_{l=1}^L \vartheta_l \mathbf{D}_{l,p} \quad (19)$$

The last part in (19) can be approximated as normally distributed complex random variable with zero mean and variance $\|\mathbf{D}_p\|_2^2 \sigma_v^2$. Since $\mathbf{C}_{l,k_m} \in [+1, -1]$, we can write $\mathbb{E}\left(\sum_{l=1}^L \sum_{m=1}^M \lambda_{l,m} \mathbf{C}_{l,k_m} \mathbf{D}_{l,p}\right) = 0$. Moreover, using the derivation in Appendix-A, we can assume $\sigma_r \approx \sigma_i$. By using the central limit theorem, the distribution of real and imaginary parts of $\sum_{l=1}^L \sum_{m=1}^M \lambda_{l,m} \mathbf{C}_{l,k_m} \mathbf{D}_{l,p}$ can be approximated by two zero-mean uncorrelated random variables having normal distributions with the same variance $M \|\mathbf{D}_p\|_2^2 \sigma_r^2$. Hence, the complex quantity $\mathbf{D}_p^T \mathbf{y}$ can be characterize complex random variables with zero mean and variance $2M \|\mathbf{D}_p\|_2^2 \sigma_r^2 + \|\mathbf{D}_p\|_2^2 \sigma_v^2$. Thus, under the hypothesis \mathcal{H}_0 , $\mathbf{D}_p^T \mathbf{y}$ can be modeled as a Rayleigh distribution with mode $\sigma_{0,p} = \sqrt{M \|\mathbf{D}_p\|_2^2 \sigma_r^2 + \|\mathbf{D}_p\|_2^2 \sigma_v^2}$. Now, for a particular value of $\xi_p : p \in \{1, 2, \dots, M\}$, the probability of false alarm for the p^{th} correlation be

$$P_f^{(p)} = P\left(|\mathbf{D}_p^T \mathbf{y}| > \xi_p | \mathcal{H}_0\right) \quad (20)$$

Note that, the random variable $\mathbf{D}_p^T \mathbf{y}$ has a Rayleigh distribution. Hence, its CDF can be defined as

$$F(z) = P\left(|\mathbf{D}_p^T \mathbf{y}| \leq z\right) = 1 - e^{-z^2/2\sigma_0^2} \quad (21)$$

Then (20) becomes

$$P_f^{(p)} = P\left(|\mathbf{D}_p^T \mathbf{y}| > \xi_p | \mathcal{H}_0\right) = e^{-\xi_p^2/2\sigma_0^2} \quad (22)$$

Thus, for a desired probability of false alarm ϕ , we have

$$\xi_p = \sigma_{0,p} \sqrt{-2 \log(\phi)}. \quad (23)$$

On the other hand, if \mathcal{H}_1 is true, then (9) follows

$$\mathbf{D}_p^T \mathbf{y} = 1 - \sum_{l=1}^L \sum_{m=1}^M \lambda_{l,m} \mathbf{C}_{l,k_m} \mathbf{D}_{l,p} + \sum_{l=1}^L \vartheta_l \mathbf{D}_{l,p} \quad (24)$$

The quantity $|\mathbf{D}_p^T \mathbf{y}|$ can be described by a random variable having Rician distribution with parameters $\mu = 1$ and $\sigma = \sigma_{0,p}$. Thus, for a particular threshold ξ_p , the detection probability for p^{th} correlation can be calculated as

$$\begin{aligned} P_d^{(p)} &= P\left(|\mathbf{D}_p^T \mathbf{y}| > \xi_p | \mathcal{H}_1\right) \\ &= Q_1\left(\frac{1}{\sigma_{0,p}}, \frac{\xi_p}{\sigma_{0,p}}\right) \end{aligned} \quad (25)$$

where $Q_1(\cdot, \cdot)$ is the Marcum-Q function.

Remark 2. The value of $\sigma_{0,p}$ can control the false alarm rate and the probability of detection. A large value of $\sigma_{0,p}$ increases the noise contribution in the signal, and hence, the false alarm rate (see (22)). On the other hand, the value of $\sigma_{0,p}$ depends on the value of $\|\mathbf{D}_p\|_2^2$. Hence, in a particular environment, the code detection probability of a user increases if it can select a code with lower $\|\mathbf{D}_p\|_2^2$. Another interesting observation is that if we set a fixed false alarm rate ϕ in (23) for every $p = 1, 2, \dots, K$, we may get K different values of threshold $\{\xi_p\}_{p=1}^K$, each for a specific column of \mathbf{D}_p , and hence, the detection rate computed in (25) may have K different values. For illustration purpose, we set $\bar{P}_d^{(p)} = \frac{1}{K} \sum_{p=1}^K P_d^{(p)}$ in (18) to compute the overall detection probability.

Remark 3. Equation (16) requires the total number of active devices M which is unknown in practice. The energy received at BS due to real parts of \mathbf{y} be (using (6))

$$\mathcal{G} = \Re(\mathbf{y})^T \Re(\mathbf{y}) = \sum_{\ell=1}^L \left[\sum_{m=1}^M \left\{ \mathbf{C}_{\ell,k_m} - \lambda_{\ell,m}^{(\Re)} \mathbf{C}_{\ell,k_m} \right\} + v_{\ell}^{(\Re)} \right]^2 \quad (26)$$

where $v_{\ell}^{(\Re)}$ is the real part of v_{ℓ} and $v_{\ell}^{(\Re)} \sim \mathcal{N}(0, \sigma_v^2/2)$. Then $\sum_{k=1}^L \left(v_k^{(\Re)}\right)^2$ can be described as a random variable with Chi-square distribution having mean $L\sigma_v^2/2$ and variance $L\sigma_v^4/4$. Furthermore, for large L , using central limit theorem it can be shown that the quantity can be approximated as a normally distributed variable with mean $L\sigma_v^2/2$ and variance $L\sigma_v^4/4$. Then after a few computations it can be verified that

$$\mathbb{E}(\mathcal{G}) = ML - 2ML\mathbb{E}(\lambda^{(\Re)}) + ML\mathbb{E}\left(\left(\lambda^{(\Re)}\right)^2\right) + L\sigma_v^2/2, \quad (27)$$

where $\mathbb{E}(x)$ is mathematical expectation of x . Hence, one can estimate the value of M from $\Re(\mathbf{y})^T \Re(\mathbf{y})$.

III. DIFFERENTIATED RANDOM ACCESS

In a Smart Grid communications environment, it is expected that the number of low priority M2M devices (e.g., meters and sensors) would be much higher than that of the high priority devices (e.g., controllers and relays). As a result, an increase in the low priority random access requests may increase the access delay of the high priority requests resulting into QoS-degradations for the time-critical M2M applications. The aim of the differentiated random access procedure is to provide a mechanism so that the high and the low priority requests can be served separately over the same BR channel.

First, consider the simple case where 2 classes of M2M traffic exists - high and low. Let us construct the code matrix described in the previous section as:

$$\mathbf{C} = \begin{bmatrix} \mathbf{C}_G & \mathbf{0}_{G \times W} \\ \mathbf{0}_{W \times G} & \mathbf{C}_W \end{bmatrix}, \quad (28)$$

where $\mathbf{0}_{W \times G}$ is a null matrix of size $W \times G$, $\mathbf{C}_G \in \mathbb{R}^{G \times G}$ and $\mathbf{C}_W \in \mathbb{R}^{W \times W}$ are the two partial Hadamard code-matrices for high and low priority classes respectively. Thus, the original $K = L$ codes are divided into two groups such that the first G codes are assigned to the N_G high-priority stations where $N_G > G$, and the last W codes are assigned to the N_W low-priority stations, where $K = G + W$. When multiple devices access the BR channel, class-wise detection can be performed by considering $\mathbf{D}_G = (\mathbf{C}_G)^{-1}$ and $\mathbf{D}_W = (\mathbf{C}_W)^{-1}$. Thus, the received signal from the two classes of traffic would be separated at the BS, and thereby, eliminate the inter-class MAI. As a result, detection process can be carried out for \mathbf{D}_G and \mathbf{D}_W independently.

IV. SIMULATION & RESULTS

To evaluate the performance of the proposed random access scheme, we develop a Monte-Carlo simulation model using MATLAB. The simulation parameters are chosen based on the IEEE 802.16-2009 standard [8]. The system is assumed to

Table I. Multipath Channel Parameters

Parameters	SUI-3 Model			SUI-4 Model		
	Tap 1	Tap 2	Tap 3	Tap 1	Tap 2	Tap 3
Delay (μ s)	0	0.4	0.9	0	1.5	4
Power (dB)	0	-5	-10	0	-4	-8
Doppler	0.4	0.3	0.5	0.2	0.15	0.25
K-factor	1	0	0	0	0	0

be operating at 2.3 GHz with a bandwidth of 5 MHz and a sampling frequency of 5.6 MHz. The FFT size is assumed to be 512 with a cyclic-prefix size of 128 samples. To simulate multipath channels, the Stanford University Interim (SUI) channel model 3 and 4 are used as recommended by the IEEE 802.16p evolution methodology document [12]. Each of these models has three taps as listed in Table I, considering an omnidirectional BS. Additionally, the tap delays are varied based on a Chi-square distribution to make sure that each user experience a different channel in every WiMAX frame. In addition, a raised-cosine filter is used for OFDM pulse-shaping with a roll-off factor of 0.22.

We evaluate the code detection performance under each of the two different code matrices. Only SUI-3 channel model is used for this set of simulations. We follow the direction of [11] and set $\alpha = e^{i\theta}$, where $\theta = 5^0$. The ROC curve for different users by applying pseudo-random matrix is shown in Figure 1(a). For a fixed number of users M , we produce the curves in the following way: i) set an elementary false alarm ϕ and by using (15) compute the corresponding threshold ξ_ϕ ; ii) use the ξ_ϕ to produce theoretical overall probability of false alarm (using (16)) and theoretical probability of detection (using (18)); iii) generate 500 different received signals \mathbf{y} under the simulation environment described earlier; iv) for every \mathbf{y} perform the correlation as in (9); v) the correlation output is checked with the threshold ξ_ϕ to compute empirical probability of false alarm and detection rate; vi) repeat procedures i)-v) for different values of ϕ . A similar strategy is applied in obtaining Figure 1(b), which exhibits the ROC curve for the partial Hadamard code matrix.

From the results in Figure 1, we see that under both code matrices, the probability of detection increases when we increase the false alarm rate. Moreover, although the default pseudo-random matrix has more available codes (i.e. $K = 256$) than the Hadamard code matrix (i.e. $L=144$), the Hadamard code matrix significantly outperforms the pseudo-random code matrix at a given probability of false alarm. This is because the Hadamard matrix provides perfectly orthogonal codes, and the effect of MAI is mitigated during the cross-correlation of \mathbf{y} and $\mathbf{C}_p : p \in \{1, 2, \dots, K\}$. This also allows segmentation of the code matrix, as described in Section II; thereby, able to provide differentiated access.

Next, we evaluate the effect of channel noise on the code detection performance by two coding matrices in Figure 2. The simulations are conducted using both SUI-3 and SUI-4 channel models. Let the average channel power be P . Then channel SNR is defined as $\text{SNR} = 10 \log_{10}(P/\sigma_n^2)$. We fixed $\phi = 0.05$, and calculate $\xi^{(p)}$ by using (15) and (23). The values of $\xi^{(p)}$ are used as threshold for hypothetical test. From the results, we

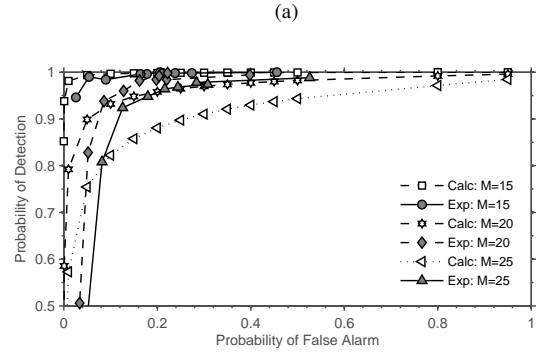
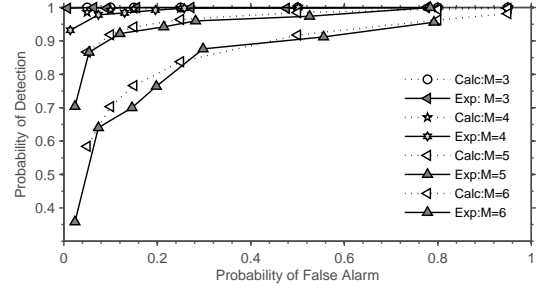


Fig. 1. Theoretical (Calc) and empirical (Exp) ROC curve for different active users (M) for (a) pseudo-random and (b) Hadamard code matrices under the SUI-3 channel model.

see that under both of the matrices, as the SNR value increases, the probability of detection increases. However, the Hadamard code matrix clearly outperforms the pseudo-random matrix irrespective of the SNR values. The results are consistent for both channel models.

V. CONCLUSION

In this paper, we presented an enhanced random access scheme for the M2M communications traffic in the Smart grid based on frequency domain pre-equalization in the physical layer. The performance of the proposed scheme was demonstrated through a comprehensive set of theoretical analysis and simulation results under two different code matrices at varying number of active users and channel conditions. The proposed scheme is fully compliant with the existing WiMAX specifications, except it requires a dedicated BR channel when both M2M and conventional applications need to be supported. Such a requirement is reasonable considering the volume of the M2M devices per BS and has already been provisioned in the IEEE 802.16p amendment. We believe that the proposed random access scheme would be able to significantly improve the performance and utilization of a WiMAX network under the Smart Grid communications environment.

APPENDIX A: MATHEMATICAL VARIANCE OF λ

Let the covariance matrix of $[\lambda_r, \lambda_i]^T$ be

$$\mathcal{V}(\lambda_r, \lambda_i) = \begin{bmatrix} \sigma_r^2 & \sigma_{ri} \\ \sigma_{ri} & \sigma_i^2 \end{bmatrix}, \quad (29)$$

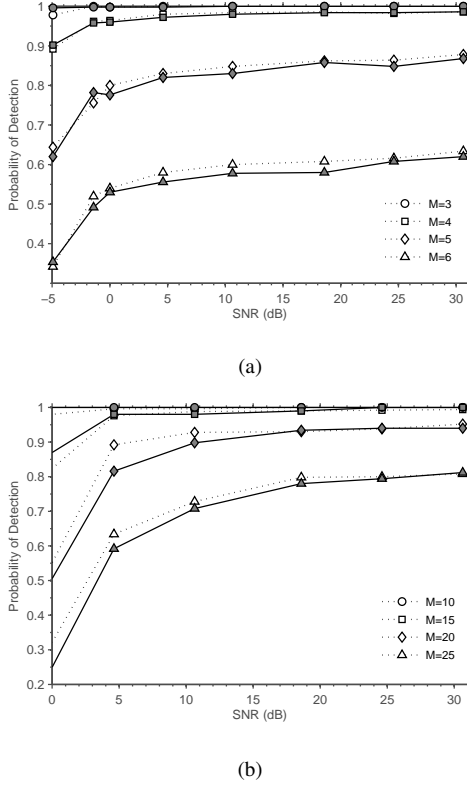


Fig. 2. Detection performance as a function of channel SNR for (a) pseudo-random and (b) Hadamard code matrices under the SUI-3 (dotted line) and SUI-4 (solid line) channel models. Distribution parameters are $\sigma_e = 0.05, \sigma_\eta = 0.05$.

where $\sigma_r^2 = \mathbb{E}(\lambda_r^2) - (\mathbb{E}(\lambda_r))^2$, $\sigma_{ri} = \mathbb{E}(\lambda_r \lambda_i) - \mathbb{E}(\lambda_r)\mathbb{E}(\lambda_i)$, and $\mathbb{E}(x)$ denotes the mathematical expectation of x . Then $\mathbb{E}(\lambda_r)$ can be calculated as

$$\mathbb{E}(\lambda_r) = \int_{-\infty}^{\infty} \int_{-\infty}^{\infty} \lambda_r f(\lambda_r, \lambda_i) d\lambda_r d\lambda_i \quad (30)$$

We evaluate the integral in polar coordinate. Let

$$\begin{aligned} \gamma &= \sqrt{\frac{(1 - \rho_r^2 - \rho_i^2)\sigma_u^2}{\sigma_v^2}}; \\ \lambda_i &= r \sin \theta - \frac{\rho_i \sigma_u}{\sigma_v}, \quad \lambda_r = r \cos \theta + \frac{\rho_r \sigma_u}{\sigma_v}; \\ \hat{\alpha} &= \frac{\rho_r \sigma_u}{\sigma_v}, \quad \beta = \frac{-\rho_i \sigma_u}{\sigma_v}, \quad \Gamma = \frac{(1 - |\rho|^2)\sigma_u^2}{\pi \sigma_v^2} \end{aligned} \quad (31)$$

Then by combining (30) and (31) we have

$$\begin{aligned} \mathbb{E}(\lambda_r) &= \Gamma \int_0^{2\pi} \int_0^{\infty} \left(\frac{r^2 \cos \theta}{(r^2 + \gamma^2)^2} + \frac{r \hat{\alpha}}{(r^2 + \gamma^2)^2} \right) dr d\theta \\ &= \Gamma \int_0^{2\pi} \left[-\left(\frac{\pi}{4\gamma} \right) \cos \theta + \frac{\hat{\alpha}}{2\gamma^2} \right] d\theta \\ &= \frac{\Gamma \pi \hat{\alpha}}{\gamma^2} = \hat{\alpha} \end{aligned} \quad (32)$$

Next we compute $\mathbb{E}(\lambda_r^2)$,

$$\mathbb{E}(\lambda_r^2) = \int_{-\infty}^{\infty} \int_{-\infty}^{\infty} \lambda_r^2 f(\lambda_r, \lambda_i) d\lambda_r d\lambda_i \quad (33)$$

Using the similar conversion in (31), we have

$$\begin{aligned} \mathbb{E}(\lambda_r^2) &= \Gamma \int_0^{2\pi} \int_0^{\infty} \left(\frac{r^3 \cos^2 \theta}{(r^2 + \gamma^2)^2} + \frac{2\hat{\alpha}r^2 \cos \theta}{(r^2 + \gamma^2)^2} + \frac{r \hat{\alpha}^2}{(r^2 + \gamma^2)^2} \right) dr d\theta \\ &= \Gamma \int_0^{2\pi} \int_0^{\infty} \left(\frac{r^3 \cos^2 \theta}{(r^2 + \gamma^2)^2} \right) dr d\theta + \frac{\Gamma \pi \hat{\alpha}^2}{\gamma^2} \\ &= \Gamma \int_0^{2\pi} \int_0^{\infty} \left(\frac{r^3 \cos^2 \theta}{(r^2 + \gamma^2)^2} \right) dr d\theta + \hat{\alpha}^2 \end{aligned} \quad (34)$$

There is no closed form solution of the first integral term. In fact, the solution become unbounded when $r \rightarrow \infty$. However, it can be bounded by some fixed value of $r < \infty$. In practice σ_h is bounded and $\sigma_h > \sigma_e, \sigma_\eta$, hence there is very low probability of (λ_r, λ_i) taking very large magnitude. An approach to obtain a reliable bound of (λ_r, λ_i) would be to use Monte Carlo simulations. With such an approach, one can simulate a large number of realizations of the variable λ according to (7), and then estimate the probability distribution function of $f(\lambda_r, \lambda_i)$. The accuracy of the distribution function increases as more number of simulations are performed. Moreover, one can plot the distribution function with respect to (λ_r, λ_i) , and thus, the bound of (λ_r, λ_i) can be estimated from the boundary of the distribution function within which 99.9% energy resides. Similarly one can evaluate

$$\mathbb{E}(\lambda_i^2) = \Gamma \int_0^{2\pi} \int_0^{\infty} \left(\frac{r^3 \sin^2 \theta}{(r^2 + \gamma^2)^2} \right) dr d\theta + \beta^2 \quad (35)$$

Finally, one can verify that

$$\mathbb{E}(\lambda_r \lambda_i) = \int_{-\infty}^{\infty} \int_{-\infty}^{\infty} \lambda_r \lambda_i f(\lambda_r, \lambda_i) d\lambda_r d\lambda_i = \beta \hat{\alpha}. \quad (36)$$

REFERENCES

- [1] "Machine-to-Machine (M2M) communications study report," *IEEE 802.16 Broadband Wireless Access Working Group*, 2010.
- [2] N. Himayat, S. Talwar, K. Johansson, S. Andreev, O. Galinina, and A. Turlikov, "IEEE 802.16p Performance requirements for network entry by large number of devices," *IEEE 802.16p Working Group*, 2010.
- [3] J. Krinock, M. Singh, M. Paff, A. Lonkar, L. Fung, and C. Lee, "Comments on OFDMA ranging scheme described in IEEE 802.16 ab-01/01r1," *document IEEE*, vol. 802, 2001.
- [4] "IEEE Standard for Air Interface for Broadband Wireless Access Systems—Amendment 1: Enhancements to Support Machine-to-Machine Applications," *IEEE Std 802.16p-2012*, pp. 1–82, 2012.
- [5] H. Wu, C. Zhu, R. J. La, X. Liu, and Y. Zhang, "FASA: Accelerated S-ALOHA using access history for event-driven M2M communications," *Networking, IEEE/ACM Transactions on*, vol. PP, no. 99, pp. 1–1, 2013.
- [6] Y. Liu, C. Yuen, J. Chen, and X. Cao, "A scalable Hybrid MAC protocol for massive M2M networks," in *Wireless Communications and Networking Conference (WCNC), 2013 IEEE*, 2013, pp. 250–255.
- [7] J. B. Andersen, J. O. Nielsen, G. F. Pedersen, G. Bauch, and G. Dietl, "Doppler spectrum from moving scatterers in a random environment," *Wireless Communications, IEEE Transactions on*, vol. 8, no. 6, pp. 3270–3277, 2009.
- [8] "IEEE standard for local and metropolitan area networks," *IEEE802.16-2009*, pp. 1–2080, 2009.
- [9] D. G. Jeong and M.-J. Kim, "Effects of channel estimation error in MC-CDMA/TDD systems," in *Vehicular Technology Conference (VTC), 2000 IEEE 51st*, vol. 3, 2000, pp. 1773–1777.
- [10] K. Fazel and S. Kaiser, *Multi-carrier and spread spectrum systems: from OFDM and MC-CDMA to LTE and WiMAX*. Wiley. com, 2008.
- [11] R. Baxley, B. Walkenhorst, and G. Acosta-Marum, "Complex Gaussian ratio distribution with applications for error rate calculation in fading channels with imperfect CSI," in *Global Telecommunications Conference (GLOBECOM 2010), 2010 IEEE*, Dec 2010, pp. 1–5.
- [12] "IEEE 802.16p Machine to Machine (M2M) Evaluation Methodology Document," *IEEE 802.16 Broadband Wireless Access Working Group*, 2011.